



Full length article

Degradation, intra-articular retention and biocompatibility of monospheres composed of [PDLLA-PEG-PDLLA]-b-PLLA multi-block copolymers



Maria J. Sandker^{a,*}, Luisa F. Duque^b, Everaldo M. Redout^c, Alan Chan^d, Ivo Que^e, Clemens W.G.M. Löwik^e, Evelien C. Klijnstra^b, Nicole Kops^a, Rob Steendam^b, Rene van Weeren^c, Wim E. Hennink^f, Harrie Weinans^{g,h}

^a Department of Orthopaedics, Erasmus Medical Center, P.O. Box 2040, 3000 CA Rotterdam, The Netherlands

^b InnoCore Pharmaceuticals, L.J. Zielstraweg 1, 9713 GX Groningen, The Netherlands

^c Department of Equine Sciences, Faculty of Veterinary Medicine, Utrecht University, P.O. Box 80163, 3508 TD Utrecht, The Netherlands

^d Percuros B.V., P.O. Box 217, 7500 AE Enschede, The Netherlands

^e Department of Radiology, Leiden University Medical Center, P.O. Box 9600, 2300 RC Leiden, The Netherlands

^f Department of Pharmaceutics, Utrecht Institute for Pharmaceutical Sciences, Utrecht University, Postbus 80082, 3508 TB Utrecht, The Netherlands

^g Department of Orthopaedics and Department of Rheumatology, UMC Utrecht, P.O. Box 85500, 3508 GA Utrecht, The Netherlands

^h Department of Biomechanical Engineering TUDelft, Mekelweg 2, 2628 CD Delft, The Netherlands

ARTICLE INFO

Article history:

Received 24 May 2016

Received in revised form 2 October 2016

Accepted 1 November 2016

Available online 2 November 2016

Keywords:

Monodisperse microspheres

Intra-articular

Anti-inflammatory

Biocompatibility

Biodegradable polymers

ABSTRACT

In this study, we investigated the use of microspheres with a narrow particle size distribution ('monospheres') composed of biodegradable poly(DL-lactide)-PEG-poly(DL-lactide)-b-poly(L-lactide) multiblock copolymers that are potentially suitable for local sustained drug release in articular joints. Monospheres with sizes of 5, 15 and 30 µm and a narrow particle size distribution were prepared by a micro-sieve membrane emulsification process. During *in vitro* degradation, less crystallinity, higher swelling and accelerated mass loss during was observed with increasing the PEG content of the polymer. The monospheres were tested in both a small (mice/rat) and large animal model (horse). *In vivo* imaging after injection with fluorescent dye loaded microspheres in mice knees showed that monospheres of all sizes retained within the joint for at least 90 days, while the same dose of free dye redistributed to the whole body within the first day after intra-articular injection. Administration of monospheres in equine carpal joints caused a mild transient inflammatory response without any clinical signs and without degradation of the cartilage, as evidenced by the absence of degradation products of sulfated glycosaminoglycans or collagen type 2 in the synovial fluid. The excellent intra-articular biocompatibility was confirmed in rat knees, where µCT-imaging and histology showed neither changes in cartilage quality nor quantity. Given the good intra-articular retention and the excellent biocompatibility, these novel poly(DL-lactide)-PEG-poly(DL-lactide)-b-poly(L-lactide)-based monospheres can be considered a suitable platform for intra-articular drug delivery.

Statement of Significance

This paper demonstrates the great potential in intra-articular drug delivery of monodisperse biodegradable microspheres which were prepared using a new class of biodegradable multi-block copolymers and a unique membrane emulsification process allowing the preparation of microspheres with a narrow particle size distribution (monospheres) leading to multiple advantages like better injectability, enhanced reproducibility and predictability of the *in vivo* release kinetics. We report not only on the synthesis and preparation, but also *in vitro* characterization, followed by *in vivo* testing of intra-articular biocompatibility of the monospheres in both a small and a large animal model. The favourable intra-articular biocompatibility combined with the prolonged intra-articular retention (>90 days) makes these monospheres an interesting drug delivery platform. What should

* Corresponding author at: Erasmus MC, University Medical Centre, Department of Orthopaedics, Room Ee16-14, P.O. Box 2040, 3000 CA Rotterdam, The Netherlands.

E-mail addresses: m.sandker@erasmusmc.nl (M.J. Sandker), luisa.duque@fu-berlin.de (L.F. Duque), e.redout@uu.nl (E.M. Redout), achan@percuros.com (A. Chan), l.que@lumc.nl (I. Que), c.w.g.m.lowik@lumc.nl (C.W.G.M. Löwik), klijnstra@innocorepharma.com (E.C. Klijnstra), n.kops@erasmusmc.nl (N. Kops), r.steendam@innocorepharma.com (R. Steendam), r.vanweeren@uu.nl (R. van Weeren), w.e.hennink@uu.nl (W.E. Hennink), h.h.weinans@umcutrecht.nl (H. Weinans).

also be highlighted is the use of horses; a very accurate translational model for the human situation, making the results not only relevant for equine healthcare, but also for the development of novel human OA therapies.

© 2016 Published by Elsevier Ltd on behalf of Acta Materialia Inc.

1. Introduction

To this date, disease modifying drugs are not available for the treatment of OA (osteoarthritis), the most common joint disease [1] and the current treatment is mainly based on pain prevention/reduction with orally administered drugs, often non-steroidal anti-inflammatory drugs (NSAIDs) [2]. Due to the chronic nature of OA in combination with the short half-life and poor distribution of drugs in general, and in this case more specifically NSAIDs to the joint [3–5], oral medication has to be taken daily for a long period and in high dosages. This high systemic exposure can in its turn lead to unwanted side-effects [2,6]. To circumvent these adverse effects, intra-articular injections (mainly hyaluronan or corticosteroids) have been used quite extensively in clinical practice, but this route of drug delivery has as a major drawback that the injected substance is rapidly released from the joint with daily synovial fluid turnover [7–9], making multiple injections necessary [7]. Ideally, a single intra-articular injection of a local drug delivery system (DDS) for OA would provide sustained drug concentrations in the injected joint in a controlled way for a longer period of action. Drug delivery systems can significantly improve pharmacokinetics of therapeutic compounds, which is especially relevant for the treatment of chronic diseases and for compounds with a narrow therapeutic window, since systemic plasma concentrations can be reduced with concurrent reduction of undesirable side-effects [10,11]. Moreover, the use of registered drugs and drug candidates, which generally are inactivated and eliminated from the body before even entering the joint, would benefit for therapeutic outcome when administered locally to the tissue of interest. Biodegradable DDSs are attractive for clinical applications since their degradation products are eliminated via metabolic routes and/or excreted by the kidneys, obviating the need for surgical removal. To date, several biodegradable DDSs for intraarticular delivery have been developed, including liposomes, hydrogels and polymeric nano/microparticles [12–15]. Poly(DL-lactide) (PDLLA) and poly(DL-lactide-co-glycolide) (PLGA) are the most widely used biodegradable polyesters for use in sustained release microparticles. However, a limitation of PDLLA and PLGA is that acidic degradation products that are formed upon hydrolysis of the ester bonds accumulate in the polymer matrix due to which the in situ pH in the microparticles may drop significantly [16,17]. The acidic micro-environment has been reported to negatively impact the stability of pH sensitive therapeutic agents such as proteins [18] and cause irregular release profiles of encapsulated actives [19] as well as dose-dumping of acidic degradation products which may evoke significant foreign body reactions [20]. Controllable and sustained drug release has been observed with microparticle-based systems prepared by different manufacturing processes [12,21], where emulsification/solvent evaporation is the most commonly used method [22–24]. Nevertheless, the difficulty to control particle size with this technique and the broad particle size distribution of the obtained microspheres leads to difficulties in formulation reproducibility and poor injectability [25,26].

Microsieve membrane emulsification allows the preparation of uniformly sized particles with average size ranging from tens of nanometers to several hundreds of micrometers [27,28]. The advantages of membrane emulsification include 1) excellent

control over the particle size and narrow particle size distribution and 2) mild process conditions as no shear forces are needed to form the droplets. Due to the absence of coarse particles, which could potentially block the injection needle, monospheres can be administered less painfully compared to polydisperse microspheres since smaller injection needles can be used [25,29]. Monospheres also lack the presence of a fraction of very small microspheres which can induce particle-induced immunoactivation [25]. Furthermore, size uniformity enables the microspheres to deliver a more precise amount of drug per microsphere, optimization of the drug release kinetics and hence more reproducible and predictable *in vivo* pharmacokinetics [30,31]. The Shirasu Porous Glass (SPG) membranes have been widely used to prepare uniformly sized microparticles [32]. Microsieve™ emulsification is an alternative membrane emulsification technique preparation of monodisperse microspheres (monospheres™) [33]. Contrary to other membrane-based droplet and particle production methods, the droplet size (and thus the particle size) is solely determined by the membrane design and independent of other process parameters. As a consequence, scalability of the process is straightforward and can be achieved by simply increasing the number of pores of the microsieve membrane or by adding more microsieves to the process.

In the present study we used a series of novel phase separated poly(DL-lactide)-PEG-poly(DL-lactide)-*b*-poly(L-lactide) multi-block copolymers ([PDLLA-PEG-PDLLA]-*b*-PLLA) obtained by polymer chain extension of telechelic poly(L-lactide) diol (PLLA) and poly(DL-lactide)-PEG-poly(DL-lactide) diol (PDLLA-*b*-PEG-*b*-PDLLA) with 1,4-butanediisocyanate [34]. To prepare microspheres with a narrow size distribution ('monospheres') by means of microsieve membrane emulsification. By varying the ratio of the rigid, semi-crystalline poly(L-lactide) blocks (PLLA) and the soft amorphous poly(DL-lactide)-PEG-poly(DL-lactide) blocks, the hydrophilicity and swelling degree of these multi-block copolymers can be tailored, which allows control over drug release kinetics. Drug release from [PDLLA-PEG-PDLLA]-*b*-PLLA multi-block copolymers is generally controlled by diffusion through the swollen polymer network, which is in contrast to PDLLA and PLGA polymers, where release is in general controlled by degradation of the polymer matrix. Another advantage of the [PDLLA-PEG-PDLLA]-*b*-PLLA multi-block copolymers is that, due to swelling of the polymer matrix, acidic degradation products do not accumulate in the polymer matrix, but are released instead, leading to the preservation of a less acidic micro-environment as compared to PLGA or PDLLA polyesters.

Besides, due to the hydrophilic and swellable nature of the [PDLLA-PEG-PDLLA]-*b*-PLLA multi-block copolymers used in the present study, it is expected that acidic degradation products will not accumulate in the polymer matrix [35], which is anticipated to positively contribute to the preservation of the integrity and bioactivity of the encapsulated therapeutic agents [16,36,37].

In the current study, we investigated the suitability of monospheres composed of biodegradable [PDLLA-PEG-PDLLA]-*b*-PLLA multi-block copolymers with different block ratios as a platform for local intra-articular drug delivery. Intra-articular retention and biocompatibility of these monospheres were assessed in rodents (mice and rats) as well as horses. Like humans, horses suffer from OA, with up to 60% of equine lameness being OA-related

[38,39]. Lameness is the leading cause of economic loss in the equine industry, making effective new therapies for equine OA very valuable. Furthermore, the horse is an accurate translational model for human OA since they both develop OA spontaneously [40], with the carpal joint specifically showing much analogy to human knee OA [41,42]. This would make the results of this study not only relevant for equine healthcare, but also for the potential development of novel human OA treatment options.

2. Materials and methods

2.1. Materials

PEG standards, polyvinyl alcohol (PVA 13–23) and sodium dodecyl sulphate (SDS) were purchased from Sigma Aldrich (Zwijndrecht, The Netherlands). Carboxymethyl cellulose (CMC) was purchased from Aqualon (Barendrecht, The Netherlands). Dichloromethane (DCM, p.a. stabilized with EtOH), sodium azide (NaN₃) and Tween-20 were purchased from Across (Geel, Belgium). Ultrapure water was purchased from B. Braun Medical B.V. (Oss, The Netherlands). Mannitol was purchased from Fagron (Barbsbütel, Germany). NIR780 was purchased from Li-Cor Inc (Nebraska, USA). Lumogen F Red 300 (Perylene red) was purchased from BASF (Ludwigshafen, Germany). Hexabrix 320®, a clinical iodine-based contrast agent, was obtained from Guerget, The Netherlands. All reagents were used as received.

2.2. Polymer synthesis

SynBiosys Pro [PDLLA-PEG₁₀₀₀-PDLLA]-*b*-[PLLA] multi-block copolymers with various [PDLLA-PEG₁₀₀₀-PDLLA]/[PLLA] block ratios were synthesized by InnoCore Pharmaceuticals (Groningen, The Netherlands) as described before [34,43]. Typically, L-lactide and DL-Lactide were dried for 17 h at 50 °C under vacuum. Poly(ethylene glycol) with a molecular weight of 1000 g/mol (PEG1000) was dried for 17 h at 90 °C under vacuum. 1,4-Butanediol and 1,4-butanediisocyanate were distilled under reduced pressure. The purity of distilled 1,4-butanediol and 1,4-butanediisocyanate was confirmed by ¹H NMR (CDCl₃).

Low molecular weight poly(L-lactide) [PLLA] (Mw 4000 g/mol) and poly(DL-lactide)-polyethyleneglycol-poly(DL-lactide) [PDLLA-PEG₁₀₀₀-PDLLA] (Mw 2000 g/mol) prepolymers were synthesized by standard stannous octoate catalysed ring-opening polymerization. Typically, to prepare PLLA with a target molecular weight of 4000 g/mol, 244.37 g (1.695 mol) of L-lactide was introduced into a three-necked bottle under nitrogen atmosphere and 5.63 g (62.47 mmol) of 1,4-butanediol was added to initiate ring-opening polymerization. Stannous octoate was added at a ratio of 11500 mol/mol monomer/catalyst. The mixture was magnetically stirred for 65 h at 140 °C and subsequently cooled down to room temperature. PDLLA-PEG₁₀₀₀-PDLLA prepolymer with a target molecular weight of 2000 g/mol, was synthesized in a similar

way using 125 g (0.867 mol) of DL-lactide, 125 g (0.125 mol) of PEG₁₀₀₀ and stannous octoate at a ratio of 13500 mol/mol monomer/catalyst.

PLLA and PDLLA-PEG₁₀₀₀-PDLLA prepolymers were subsequently chain-extended with 1,4-butanediisocyanate to yield [PDLLA-PEG₁₀₀₀-PDLLA]-[PLLA] multiblock co-polymers with [PDLLA-PEG₁₀₀₀-PDLLA]/[PLLA] block ratios of 10/90, 16/84, 20/80, 30/70 and 50/50 w/w. PLLA and PDLLA-PEG₁₀₀₀-PDLLA pre-polymers were introduced into a three-necked bottle under nitrogen atmosphere. Then 65 ml of dry 1,4-dioxane (distilled over sodium wire) was added to obtain a 30 wt.% pre-polymer solution which was heated to 80 °C to dissolve the prepolymers where after 4.23 g (30.18 mmol) of 1,4-butanediisocyanate was added. The reaction mixture was stirred mechanically for 20 h, cooled down to room temperature, where after it was transferred into a tray, frozen and vacuum-dried at 30 °C to remove 1,4-dioxane. The residual 1,4-dioxane content, as measured by GC headspace, was less than 200 ppm for all multi-block co-polymers. Residual contents of stannous octoate as measured by inductively coupled plasma analysis was <200 ppm for all multi-block co-polymers. Using ¹H NMR analysis, only lactate/PEG ratios can be determined as it cannot be judged from the lactate signal in which block it resides. Hence the total LA/PEG mole/mole ratio equivalent for the block ratio is reported. In the table it can be seen that the mole/mole ratios determined by NMR are close to the mole/mole ratios based on actual prepolymer in-weights, indicating that the actual block-copolymers have a block ratio very similar to their intended block ratio (Table 1).

2.3. Polymer characterization and in vitro polymer degradation

2.3.1. Thermal properties

Thermal properties of the synthesized polymers were measured by differential scanning calorimetry (DSC) using a Q1000 differential scanning calorimeter (TA instruments, Ghent Belgium) operated in the modulated mode (±1.0 °C every 60 s) where the sample (5–10 mg) was heated from –85 to 180 °C at a rate of 5 °C/min. During the measurement, the sample cell was purged with nitrogen. The reversed heat flow was used for determination of the glass transition temperature (T_g, midpoint), while the total heat flow was used for determination of the melting temperature (maximum of endothermic peak, T_m). The heat of fusion (ΔH (J/g)) was calculated from the surface area of the melting endotherm. Temperature and heat flow were calibrated using indium. Measurements were done in a single heating run by modulated DSC.

2.3.2. Chemical polymer composition evaluation

¹H NMR was used to determine the DL-lactide/PEG (LA/PEG) monomer ratio of the multiblock copolymers after synthesis and during degradation. ¹H NMR was performed on a VXR Unity Plus NMR spectrometer (Varian, California, USA) operating at 300 MHz. The d1 waiting time was set to 20 s, and the number of

Table 1
Polymer block ratio, based on prepolymer in weight and determined by NMR.

| Polymer type | PLLA (g) | PDLLA-PEG ₁₀₀₀ -PDLLA (g) | Block ratio ^a (wt/wt) | Lactate/PEG ratio (mole/mole) | |
|---|----------|--------------------------------------|----------------------------------|-------------------------------|---------------------------------|
| | | | | In weight ^b | ¹ H NMR ^c |
| 10[PDLLA-PEG ₁₀₀₀ -PDLLA]-90[PLLA] | 119.93 | 12.83 | 9.7/90.3 | 270.4 | 258.8 |
| 16[PDLLA-PEG ₁₀₀₀ -PDLLA]-84[PLLA] | 90.34 | 17.14 | 16.0/84.0 | 156.9 | 173.4 |
| 20[PDLLA-PEG ₁₀₀₀ -PDLLA]-80[PLLA] | 88.05 | 21.84 | 19.9/80.1 | 124.7 | 126.9 |
| 30[PDLLA-PEG ₁₀₀₀ -PDLLA]-70[PLLA] | 73.52 | 30.58 | 29.4/70.6 | 81.4 | 85.8 |
| 50[PDLLA-PEG ₁₀₀₀ -PDLLA]-50[PLLA] | 48.37 | 46.91 | 49.2/50.8 | 42.9 | 46.1 |

^a [PDLLA-PEG₁₀₀₀-PDLLA]/[PLLA] block ratio based on in weight of monomers and prepolymers.

^b Molar Lactate/PEG ratio of the resulting multi-block copolymer as calculated based on in-weight of prepolymers.

^c Molar Lactate/PEG ratio of the resulting multi-block copolymer as determined from ¹H NMR.

scans was 16–32. Spectra were recorded from 0 to 14 ppm. ^1H NMR samples were prepared by dissolving 10 mg of polymer into 1 mL of deuterated chloroform (CDCl_3), and the spectrum was recorded from 0 to 8 ppm using CHCl_3 present as trace in CDCl_3 as reference. PDLLA/PEG molar ratio was calculated from the $-\text{O}-\text{CH}(\text{CH}_3)\text{C}(\text{O})-$ methine groups of PDLLA and D,L -lactide monomer at δ 5.1–5.4 and δ 5.0–5.1, respectively, and the $-\text{CH}_2\text{CH}_2-\text{O}$ methine groups of PEG at δ 3.6–3.7.

2.3.3. Molecular weight analysis

The number average molecular weight (M_n) and the weight average molecular weight (M_w) of synthesized polymers was determined using size exclusion chromatography (sEC-HPLC, Waters, Breeze, USA). Polymer samples (10 mg) were dissolved in DMF (1 mL) and PEG standards with molecular weights of 1–218 kg/mol were prepared likewise. Samples and PEG standards were injected (50 μL) onto the SEC column (Thermo Fischer, Column 1: Plgel 5 μm 500 Å, column 2: Plgel 5 μm 500 Å, column 3: Plgel 5 μm 104 Å, eluent: DMF with 0.1 M LiBr, flow 1 mL/min). Polymers were detected by refractive index. The apparent molecular weights (M_n and M_w) were then calculated with the aid of the PEG standards.

2.3.4. In vitro degradation

Polymer films with a thickness of 200–250 μm were prepared by dissolving 5 g of polymer in 45 g of DCM (10 wt.% polymer solution) and solvent casting of the solutions in Petri dishes and overnight incubation at RT to evaporate DCM followed by vacuum-drying at 50 °C for 5 days. Films were cut into 1 \times 2 cm test samples with a weight of 50–150 mg and the obtained samples were then placed in test tubes containing 10–20 mL of 100 mM PBS (82 mM Na_2HPO_4 , 18 mM KH_2PO_4 , 9 mM NaCl, and 0.2% NaN_3) pH 7.4 and incubated at 37 °C. At different time points test samples were collected, rinsed with demi-water over a 0.45 μm filter to remove buffer salts, blotted with tissue paper to remove excess of medium and weighed to determine their wet mass ($m_{\text{wet},t}$) and swelling degree (SW). After vacuum-drying over silica gel, the weight of the sample was determined again ($m_{\text{dry},t}$). The swelling degree and remaining mass were calculated as follows:

$$\text{SW} = (m_{\text{wet},t} - m_{\text{dry},t}) / m_{\text{wet},t} \quad (1)$$

$$\text{Remaining mass}(\%) = 100 \times m_{\text{dry},t} / m_{\text{dry},0} \quad (2)$$

where $m_{\text{dry},0}$ and $m_{\text{dry},t}$ are the masses of the dry sample at day 0 and dry sample at day t .

GPC and ^1H NMR measurements were performed in degraded samples as described above.

2.4. Preparation of monospheres

A membrane emulsification-based solvent extraction/evaporation process using microfabricated microsieve membranes with uniformly sized pores of 3.3 μm , 11 μm and 20 μm (Nanomi BV, The Netherlands) was used for the preparation of monospheres with target diameters of 5, 15 and 30 μm , respectively. To prepare the monospheres, approximately 0.5 g of 20[PDLLA-PEG₁₀₀₀-PDLLA]-80[PLLA] was dissolved in 1.5 mL dichloromethane (DCM) to obtain a 20% w/w solution which was subsequently filtered through a 0.2 mm PTFE filter. Using 35 mbar air-pressure, the filtered polymer solution (DP) was processed through the Microsieve membrane at an approximate rate of 0.12 mL/min into an aqueous solution containing 4% w/v PVA (CP). The CP/DP volume ratio was around 35 v/v. The formed emulsion was stirred over a period of 3 h at room temperature to extract and evaporate DCM. Hardened monospheres were collected by centrifugation at 2000 rpm for 3 min, washed twice with demiwater and twice with

0.05% w/v aqueous Tween 20 solution and finally lyophilized. Tween 20 was used to facilitate the re-dispersion of the monospheres during re-constitution in the injection medium.

For the preparation of perylene red loaded monospheres, the dye was co-dissolved with 20[PDLLA-PEG₁₀₀₀-PDLLA]-80[PLLA] (20% w/w) in a 1:100 w/w ratio, where after the monospheres were prepared using the same membranes and procedures as described above. Similarly, monospheres containing 0.5% w/w NIR-780F were prepared by co-dissolving the dye and 16[PDLLA-PEG₁₀₀₀-PDLLA]-84[PLLA] (20% w/w) in a 1:200 w/w ratio.

Prior to intra-articular injection in rats, monospheres were dispersed in freshly prepared sterile injection medium (0.4 wt.% CMC, 0.1 wt.% Tween 20 and 5.0 wt.% mannitol). For injection in mice and horses the monospheres were reconstituted in saline.

2.5. Monosphere characterization

Monospheres were visually examined by optical microscopy. Particle size was determined by dispersing 5–10 mg of monospheres in 50–100 mL of electrolyte solution (Beckman Coulter, Woerden, The Netherlands) and measuring the particle size distribution (PSD) with a Multisizer 3 Coulter Counter (Beckman Coulter, Woerden, The Netherlands) equipped with a 200 μm measuring cell. The volume average particle size (D_{50}) and coefficient of variance (CV%) were determined from the PSD.

Surface morphology of the monospheres was assessed by scanning electron microscopy (JCM-5000 Neoscope, Jeol, Germany). Freeze dried samples of monospheres were sputtered with a thin layer of gold using the JFC Neocoater (Jeol, Germany).

Residual dichloromethane content of lyophilized monospheres was determined by GC-FID using a TraceGC gas chromatograph (Thermo Finnigan, Rodano, Milan, Italy) equipped with a CombiPal headspace module (CTC Analytics AG, Zwingen, Switzerland) and an Agilent Column, DB-624/30 m/0.53 mm and using dichloromethane standards in DMSO in the range of 0–2000 ppm.

Endotoxin evaluation was performed by Limulus amoebocyte lysate assay according to the chromogenic endpoint standard procedure, with a lower limit of detection of 0.05 EU/mL [44].

2.6. Intra-articular retention of injected monospheres

All experimental procedures were approved by the Subcommittee on Research Animal Care at Leiden University Medical Center. Male FVB mice (4–8 weeks of age, from the LUMC breeding facility) were used for both experiments. Initially, the capacity of the 20 [PDLLA-PEG₁₀₀₀-PDLLA]-80[PLLA] monospheres to remain intra-articular was tested. Two mice were injected intra-articularly with 10 μL of a NIR-780F suspension in saline (10 $\mu\text{g}/\text{mL}$) while 2 other mice received a 10 μL intra-articular injection of 1% w/w NIR-780F loaded monospheres suspension in saline (1 mg /mL) using a 30 Gauge BD Micro-Fine syringe. In both groups the total amount of NIR-780F injected was of 0.10 μg . *In vivo* scans were made 24 h post-injection to check intra-articular retention and biodistribution. For the second experiment, knee joints were injected bilaterally with monospheres of different sizes (5, 15 and 30 μm ; $n = 3$ knees/size), and the intra-articular presence of monospheres was determined by fluorescence imaging of the injected knees of the mice at $t = 0$, $t = 1$ d, $t = 2$ d, $t = 6$ d, $t = 9$ d, $t = 39$ d and $t = 90$ d.

In the first experiment (free NIR-780F versus NIR-780F dye-loaded monospheres) fluorescence imaging of monospheres was performed with the Pearl Impulse (Li-cor, Lincoln, Nebraska USA). In the second experiment (differently sized monospheres) fluorescence imaging was performed with an IVIS Spectrum animal imaging system (Perkin Elmer/Caliper LifeSciences, Hopkinton, MA). For this second experiment, monospheres were loaded with perylene red. This dye was selected over NIR-780F because

detectability was superior. Scans were made while the mice were anesthetized with 1.5% of Isoflurane balanced with oxygen. After the last scan (day 90), the mice were sacrificed, overlying skin was removed and *ex vivo* scans of the knees were made to check for remaining signal. For spectral unmixing, an image cube was collected on the IVIS Spectrum with 18 narrow band emission filters (20 nm bandwidth) that assist in significantly reducing autofluorescence by the spectral scanning of filters and the use of spectral unmixing algorithms. Fluorescence regions were identified and spectrally unmixed using Living Image 4.3.1 software. Because of the 3D character of the joints, a reliable quantification of the amount of signal over time could not be made. Therefore, we present results based on whether there was still any signal detectable or not.

2.7 Intra-articular biocompatibility in horses

All experimental procedures and protocols were approved by the Utrecht University Committee on the Care and Use of Experimental Animals in compliance with Dutch legislation on experimental animal use. Due to the limited number of horses available for experiments, we only tested the 30 μm monospheres. The horses used in this experiment had clinically normal middle carpal joints (radiographically confirmed). The left middle carpal joint was injected with 3 ml saline solution (control), while the right middle carpal joint was injected with 200 mg of 30 μm monospheres suspended in 3 ml saline.

2.7.1. Lameness

Lameness examinations were conducted at 0, 8, 24, 72 h and 1, 2, 3, 4 weeks post injection, using a standardized scale of 0 to 5 [45]. Horses were monitored throughout the whole study for signs of discomfort.

2.7.2. Synovial fluid analysis

Synovial fluid was aspirated aseptically at the same time points the lameness examinations were conducted. A portion of the fluid was processed for white blood cell (WBC) count and total protein measurement. The remaining volume was centrifuged and analyzed for glycosaminoglycan (GAG) concentrations with a modified 1,9-dimethylmethylene blue dye-binding assay used previously in our laboratory [46] and collagen type 2 breakdown was measured by an antibody against a collagen type 2 epitope (C2C) as previously reported [46].

2.7.3. Synovial tissue analysis

To check the intra-articular retention of the monospheres in the equine joints, parts of the synovial tissue surrounding the third carpal bone were removed for histological analysis. After fixation in formalin, the synovial tissue was divided in two parts. The first part was used for light microscopic verification of the presence of monospheres within the synovial tissue 4 weeks after intra-articular injection. The second part was used for the same purpose using SEM.

2.8 Intra-articular biocompatibility in rats

The Animal Ethic committee of the Erasmus Medical Center, Rotterdam, The Netherlands, approved all conducted procedures. Twelve 16-week-old (400–450 g) male Wistar rats (Charles River Netherlands BV, Maastricht, The Netherlands) were housed in the animal facility of the Erasmus Medical Center, with a 12-h light-dark regimen, at 21 °C. Animals were fed standard food pellets and water *ad libitum*. Experiments started after a 2 weeks acclimatization period. Since all monospheres of different sizes were retained in the knee joint (results of IVIS studies in mice), we

choose to only test the smallest and largest monospheres. The desired amounts of monospheres (5 μm :2 mg/30 μl and 30 μm :10 mg/50 μl) were re-suspended in injection medium and injected into the left knee of the rats ($n = 12$) using a 27G syringe (Kendall, monoject). Contralateral knees were injected with the same volume of saline and served as controls. Scans of all knees were acquired at 3 different time points ($t = 0$, $t = 6\text{w}$ and $t = 12\text{w}$). Following the last scan, knees were harvested and EPIC μCT -scanning was performed [47].

2.8.1. μCT arthrography

Cartilage quality (sulphated glycosaminoglycan (sGAG) content) and quantity (thickness) was measured with *in vivo* μCT arthrography. Therefore, knees were injected with a radiographic contrast agent (Hexabrix (Hexabrix 320, Mallinckrodt, Hazelwood, MO, USA) mixed with 10 $\mu\text{g}/\text{ml}$ Epinephrine) as described previously [47,48]. Influx of Hexabrix into the cartilage correlates inversely with sGAG content [49,50]; therefore early changes in cartilage quality and quantity are measurable using *in vivo* μCT arthrography [47,48]. After injecting Hexabrix, rats were placed in a custom made scanner bed fixing the hind limb in extended position. Scans were made using an *in vivo* scanner (Skyscan model 1176, Skyscan, Kontich, Belgium) using the following scanner settings: isotropic voxelsize of 18 μm , 67 kV, 380 mA, 35 mm field of view, 1.0 mm Al filter, 0.5 rotation step over 198°, frame averaging of 2. Both knees were scanned at all 3 time points ($t = 0$, 1 and 6 weeks). Due to incomplete Hexabrix influx in some knees, a total of 7 animals were available for longitudinal analysis.

2.8.2. EPIC μCT imaging

Equilibrium partitioning of a contrast agent using μCT (EPIC- μCT) shows a strong correlation with cartilage sulphated-glycosaminoglycan (sGAG) content [51]. Following the last *in vivo* μCT scan, rats were sacrificed and knees were dissected with removal of the surrounding soft tissue. The tibiae were incubated for 24 h in a 40% Hexabrix solution at room temperature in order to achieve equilibrium between the contrast agent and the sGAG content of the cartilage [50]. After 24 h, samples were scanned using the following settings: isotropic voxelsize of 18 μm , 60 kV, 170 mA, 885 ms exposure time, 35 mm field of view, 0.5 mm Al filter, 0.8 rotation step over 198°, frame averaging of 3.

2.8.3. μCT data analysis

Obtained raw *in vivo* μCT images were converted into 3D reconstructions using the reconstruction software nRecon version 1.5 (SkyScan). With 3D Calc software segmentation into binary images [52] took place creating a mask overlaying bone and Hexabrix in the original gray value images (ImageJ; NIH, <http://imagej.nih.gov/ij/index.html>) [47]. Subsequently, regions of interest (ROIs) were drawn around the patellar cartilage (40 slices) for which attenuation and thickness were calculated. In the datasets acquired with EPIC- μCT imaging ROIs were drawn directly around the Hexabrix saturated cartilage of both the medial and lateral tibial plateau of the 3D reconstructed images. Subsequently, global segmentation took place between the cartilage and the adjacent areas (subchondral bone and air) and attenuation and volume of the cartilage were measured.

2.8.4. Histological analysis

Directly following the EPIC scans, knee joints were fixed with formalin, decalcified and embedded in paraffin. Six μm sections were prepared sagittally at 300 μm intervals and stained with Safranin-O. At different time points, the infrapatellar folds containing the synovial membrane of the knees injected with 5 μm monospheres were removed and immunostained in order to check for the presence of macrophages due to the presence of particles

<10 μm . The tissue was embedded in paraffin and cut in 6 μm sections. These sections were dewaxed and pre-treated with heat mediated antigen retrieval (Dako S1699, Glostrup, Denmark) at 90 °C for 20 min. Subsequently, sections were incubated with CD68 (1:100, Acris, Herford, Germany) for 60 min and visualized with AP link and label kit (Biogenex, Fremont, CA, USA), followed by a New Fuchsin substrate. Sections were dried overnight and mounted with Vectamount (Vector Laboratories, Burlingame, CA, USA).

2.9. Statistical analysis

Differences in μCT -data and histological scoring between the microsphere-injected knees and the contralateral knees were all calculated using type-1, two-tailed, paired T-tests. The differences between monospheres-injected knees and the osteoarthritic control group was calculated using type-1, two-tailed unpaired T-tests. For the measurement in the horse SF samples, the control and monospheres-injected joints were compared using paired T-tests at all time-points. Additionally, the longitudinal data were analyzed using a linear mixed model with post-hoc Bonferroni correction, CI 95%. All statistical tests were performed using SPSS-20. P-values <0.05 were considered statistically significant.

3. Results

3.1. Polymer synthesis and characterization

3.1.1. Polymer characterization

Block copolymers with different [PDLLA-PEG₁₀₀₀-PDLLA]/[PLLA] ratios were synthesized and their characteristics are reported in Table 2. This table shows that LA/PEG molar ratios of the xx [PDLLA-PEG₁₀₀₀-PDLLA]-yy[PLLA] multi-block copolymers were between 46 and 285 mol/mol, close to the theoretical values (Table 2). GPC was performed relative to PEG standards and the apparent molecular weight values were obtained with values ranging from 33.6 to 49.6 kDa for M_w and from 17.6 to 28.8 kDa for M_n . Differential scanning calorimetry (DSC) thermograms showed a slight decrease of the melting temperature of the polymers (from 136 °C to 123 °C) upon increasing the block ratio of PDLLA-PEG₁₀₀₀ from 10/90 to 50/50. Whereas the T_g decreased significantly from 53 °C to −5 °C. Swelling degrees (SW), as determined after 1 day of incubation, increased from 1.1 for 10[PDLLA-PEG₁₀₀₀-PDLLA]-90[PLLA] to 1.5 for 50[PDLLA-PEG₁₀₀₀-PDLLA]-50[PLLA].

3.1.2. In vitro polymer degradation

The degradation profile of films of the different polymers presented similar behavior. As shown in Fig. 1-A, mass loss followed a two-phase behavior with an initial phase where fast degradation occurred and a second phase where the mass reduction rate was lower. The polymer with the highest PEG content (50[PDLLA-PEG₁₀₀₀-PDLLA]-50[PLLA]) lost 46% of its weight after one week, whereas the polymer with the least PEG content (10[PDLLA-PEG₁₀₀₀-PDLLA]-90[PLLA]) only lost 3% during the same period of

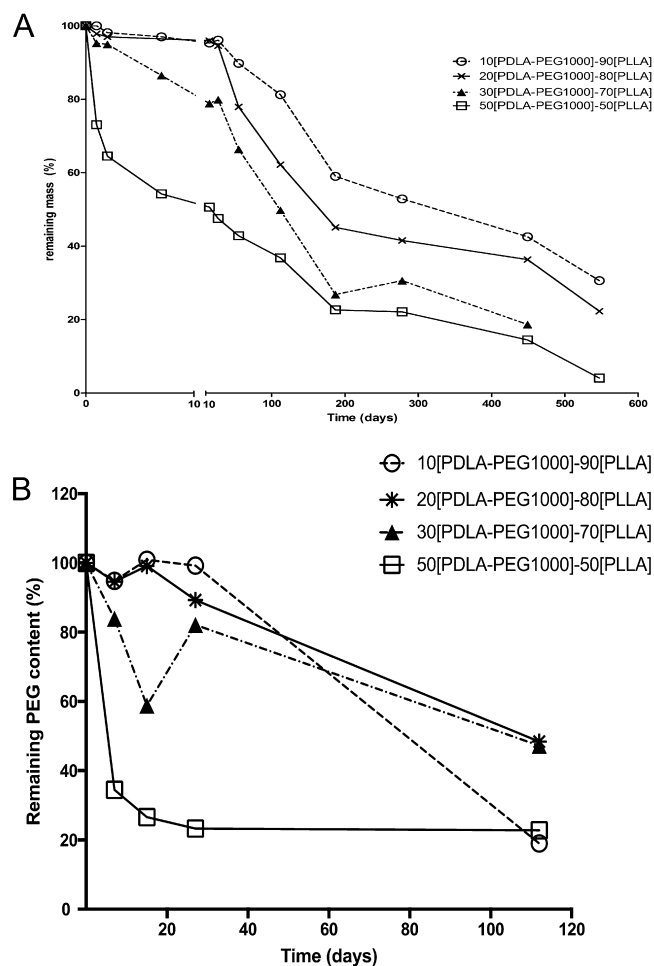


Fig. 1. A) *In vitro* degradation of xx[PDLLA-PEG₁₀₀₀-PDLLA]-yy[PLLA] multi-block copolymers expressed as remaining mass as a function of time [left] and PEG lost as a function of time [right] upon incubation in PBS, pH 7.4 and at 37 °C. B) The same degradation, expressed as PEG loss as a function of time.

time. The same behavior was observed for the PEG loss as a function of time (Fig. 1-B).

3.2. Monosphere characterization

Residual dichloromethane content of lyophilized monospheres was <600 ppm and endotoxin levels were <0.01 EU/mg, meeting the acceptance limits for parenteral injections [53]. Coulter Counter measurements indicated that the different monospheres have a narrow particle size distribution (Fig. 2-A). The average diameter (and coefficient of variance (CV)) of the differently sized monospheres were respectively 4.7 μm (CV 32.4%), 15.5 μm (CV 18.6%) and 34.4 μm (CV 12.9%). Fig. 2-B shows a SEM picture of the three different monosphere sizes, clearly visualizing their size

Table 2

Composition, PEG content, thermal properties and swelling degree of various xx[PDLLA-PEG₁₀₀₀-PDLLA]-yy[PLLA] multi-block copolymers.

| # | Polymer composition | PEG (wt%) | M_w (Da) | M_n (Da) | T_g (°C) | T_m (°C) | ΔH_m J/g | Sw (–) |
|---|---|-----------|------------|------------|------------|------------|------------------|--------|
| 1 | 10[PDLLA-PEG ₁₀₀₀ -PDLLA]-90[PLLA] | 5 | 49600 | 28800 | 51 | 136 | 67.5 | 1.1 |
| 2 | 20[PDLLA-PEG ₁₀₀₀ -PDLLA]-80[PLLA] | 10 | 33600 | 19200 | 39 | 130 | 43.9 | 1.1 |
| 3 | 30[PDLLA-PEG ₁₀₀₀ -PDLLA]-70[PLLA] | 15 | 33800 | 17600 | 21 | 129 | 35.5 | 1.2 |
| 4 | 50[PDLLA-PEG ₁₀₀₀ -PDLLA]-50[PLLA] | 25 | 46100 | 26700 | –5 | 122 | 17.5 | 1.5 |

M_w : Weight average molecular weight; M_n : Number average molecular weight; T_g : glass transition temperature; T_m : melting temperature; ΔH_m : melting enthalpy; S_w : swelling degree, as determined after 1 day of incubation.

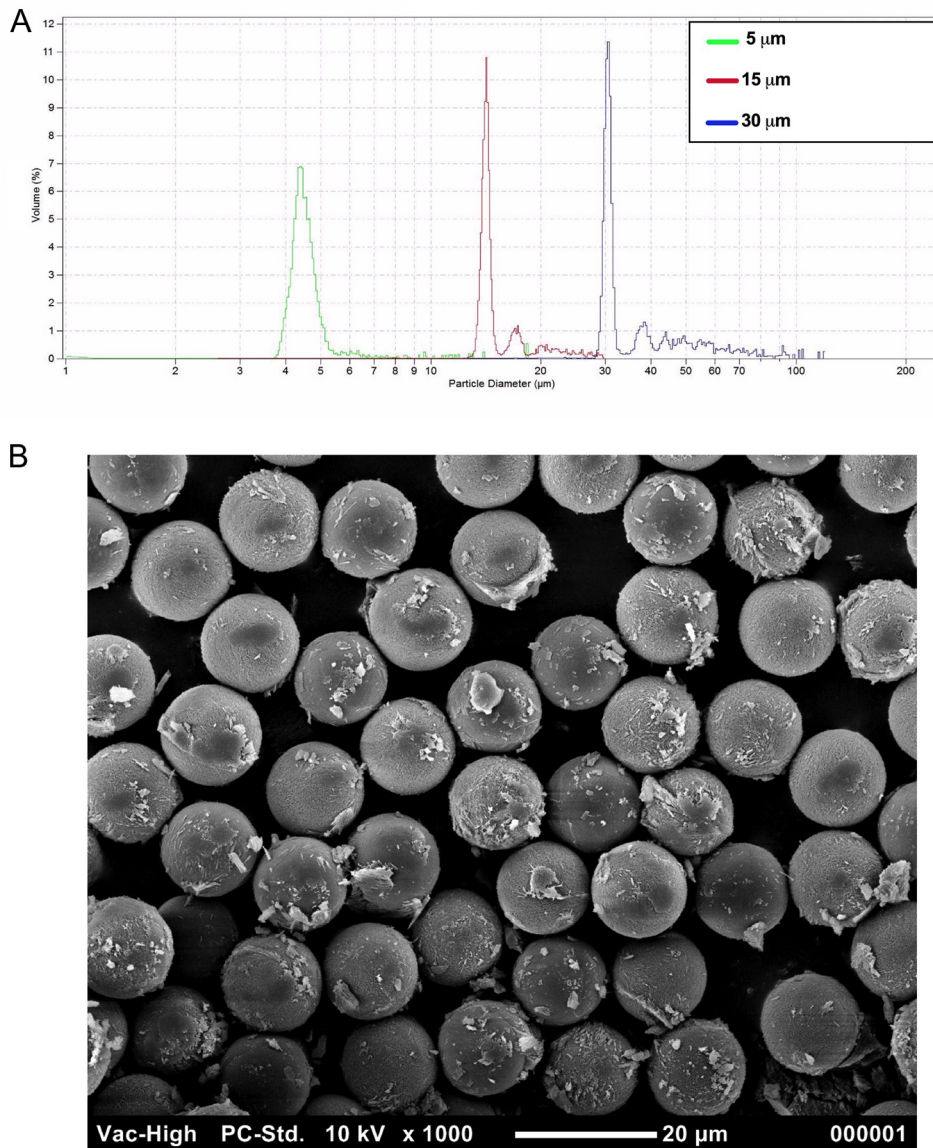


Fig. 2. A) Particle size distribution of 20[PDLLA-PEG₁₀₀₀-PDLLA]-80[PLLA] monospheres: 5, 15 and 30 μm. B) SEM picture of 15 μm 20[PDLLA-PEG₁₀₀₀]-80[PLLA] monospheres. This picture shows the size uniformity of the batches. Mannitol was used during the washing and before freezing of the monospheres, explaining the irregularities seen in the picture. The surface of the monospheres appears smooth and without pores.

uniformity and their smooth and non-porous surface (non-spherical particles correspond to mannitol particles, which was used during washing and before freeze drying of the monospheres (see [Supplementary Fig. 1](#)).

3.3. Intra-articular retention and degradation kinetics

3.3.1. Equine intra-articular monosphere retention

In vitro evaluation of the perylene red loaded monospheres was performed to ensure that the dye was not released prematurely from the 20[PDLLA-PEG₁₀₀₀-PDLLA]-80[PLLA] monospheres. Therefore, the monospheres were incubated in release buffer (100 mM phosphate buffer, pH 7.4) at 55 °C (to accelerate degradation) and the supernatant was inspected daily. The supernatant remained clear for up to 10 days, after which perylene red started to leak from the monospheres. To verify that the monospheres would retain enough perylene red during the course of the *in vivo* experiments, tissue surrounding the equine middle carpal joint was harvested 4 weeks after intra-articular injection with

peryene red loaded monospheres. In all horses parts of the tissue were red ([Fig. 3](#); left image) and upon microscopic evaluation this coloring was shown to indeed be due to the actual presence of perylene red loaded monospheres ([Fig. 3](#); middle image).

3.3.2. IVIS scanning mice

IVIS analysis of intra-articularly injected NIR-780F encapsulated in monospheres showed a distinct signal only at the site of injection, contrary to the aqueous suspension of the free fluorescent dye which quickly redistributed from the knee throughout the whole body within the first 24 h ([Fig. 4](#)). Up to 39 days, in all mice injected with perylene red-loaded monospheres, a clear signal was observed at the knee joint without re-distribution to other parts of the body. At 90 days post-injection, the signal was below detection limit in one animal only of the 5 μm monospheres group whereas in all other groups perylene fluorescence was still detected, demonstrating that at 90 days microspheres were still present. Subsequent *ex vivo* scans of the knee joints showed the presence

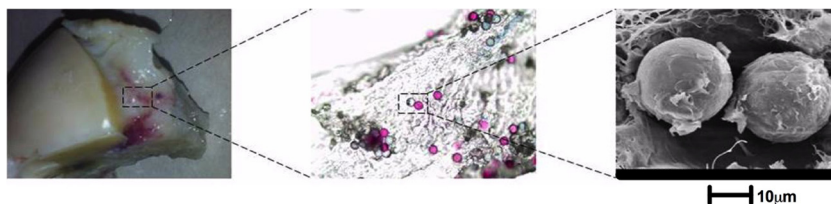
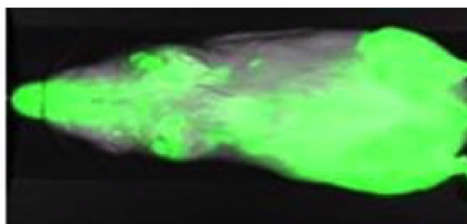
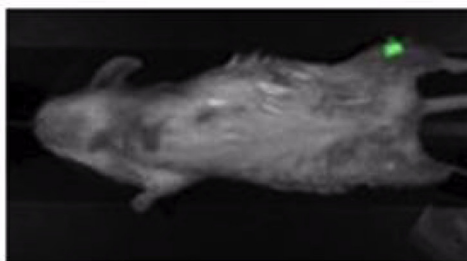


Fig. 3. Equine third carpal bone excised 4 weeks after intra articular injection of perylene red loaded monospheres. In the surrounding tissue the red dye can be easily observed (left). Microscopic images of this tissue show that the red color is indeed due to the presence of monospheres (middle). SEM pictures of these monospheres are shown on the right. (For interpretation of the references to color in this figure legend, the reader is referred to the web version of this article.)

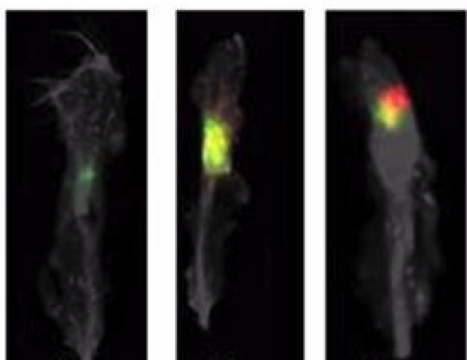
free dye
(*in-vivo* 24 hr)



microspheres
(*in-vivo* 24 hr)



microspheres
(*ex-vivo* 90 d)



5 μm

15 μm

30 μm

Fig. 4. Fluorescent images of intra-articular retention of free dye and dye-loaded monospheres in mice. Representative fluorescent images are shown for 24 h after intra-articular injection of free fluorescent dye, NIR-780F (upper picture) and monospheres (15 μm) containing the same dye (middle picture); the monospheres were able to retain the dye locally whereas the freely injected dye redistributed throughout the whole body quickly. The lower picture shows ex-vivo IVIS-scans of knees containing perylene red loaded 5 μm, 15 μm or 30 μm monospheres 90 days after injection. At this final time point, for all sizes there we still monospheres present within the knee joints.

of monospheres by remaining signal (Fig. 4) in all animals, irrespective of monosphere size.

3.4. Intra-articular biocompatibility in horses

None of the horses showed any signs of discomfort following the intra-articular injection of 30 μm 20[PDLLA-PEG₁₀₀₀-PDLLA]-80[PLLA] monospheres. Locomotion was not affected, as the lameness score for both monospheres and saline injected joints was 0 (maximum = 5) for all horses throughout the whole study.

3.4.1. Synovial fluid analysis

Intra-articular injection of unloaded monospheres led to a significant increase of WBC in the synovial fluid 8 h after injection when compared to saline injected joints (Fig. 5-A). At $t = 24$ and 72 h post injection, elevated values were still found compared to the saline-injected joint, although no significance could be found in this small group. Compared to baseline values, both saline- and monospheres injected joints showed a trend of increased WBC in the SF for a period of 72 h after the injection, which had returned to normal at one week after injection. Total protein

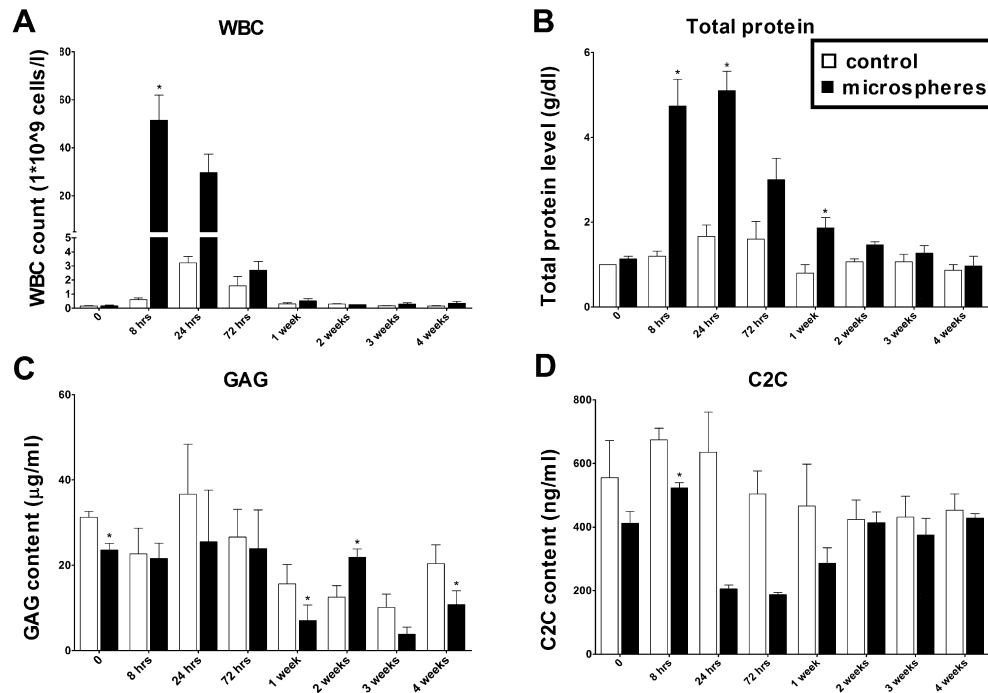


Fig. 5. Synovial fluid analysis: White Blood Cell count (A), Total protein levels (B), GAG content (C) and C2C content (D). (n = 3, control: saline injected joints, microspheres: microspheres injected joints. Values are depicted as mean \pm SD; *: $p < 0.05$ vs. control.

content (Fig. 5-B) also increased from $t = 8$ h until 1 week post injection due to the intra-articular injection of microspheres (significant differences at 8 h, 24 h and 1 week). At baseline (before injecting either saline or microspheres in the joints), a significant difference in GAG was found between the two groups. For all time points GAG release into the SF remained at or below baseline values. At some time points, significant differences were seen when compared to the control joint (saline injected) but there was not a clear trend and the phenomenon seemed to appear quite randomly. Moreover, compared to values found in a previously conducted study, our values are in the range of what is normally found in healthy joints, and a tenfold lower than values found in inflamed joints [46]. Also, Hyonate[®], which is clinically accepted and used as an intra-articular intervention for OA, is proven to give rise of the GAG-content in synovial fluid of horses 1 day after injection [54]. No increase in C2C epitope content (collagen breakdown biomarker) was found at any time point (Fig. 5-D), indicating that no significant damage to the cartilage occurred due to the intra-articular injections. A significantly lower C2C content in the

synovial fluid was detected at 8 h after microsphere injection compared to the control joints. However, there is no clear explanation for this observation and this is therefore likely due to physiological fluctuation. Moreover, comparing our values to what was found in a previously conducted study, C2C epitope in the synovial fluid remained at base-line levels showing that the differences found are indeed a fluctuation of physiological levels and not considered to be clinically significant [54].

3.5. Intra-articular biocompatibility in rats

3.5.1. *In vivo* μ CT arthrography scanning

Following the intra-articular injections, no toxic responses (e.g. changed locomotion, joint redness/swelling) occurred during the 12-weeks observation period. Arthrographies at $t = 0$ showed a small difference ($p < 0.05$) in attenuation between microsphere- and saline injected knees (Fig. 6), however this difference is not clinically relevant since it is well within the range of what is normally found for healthy cartilage and much lower than diseased

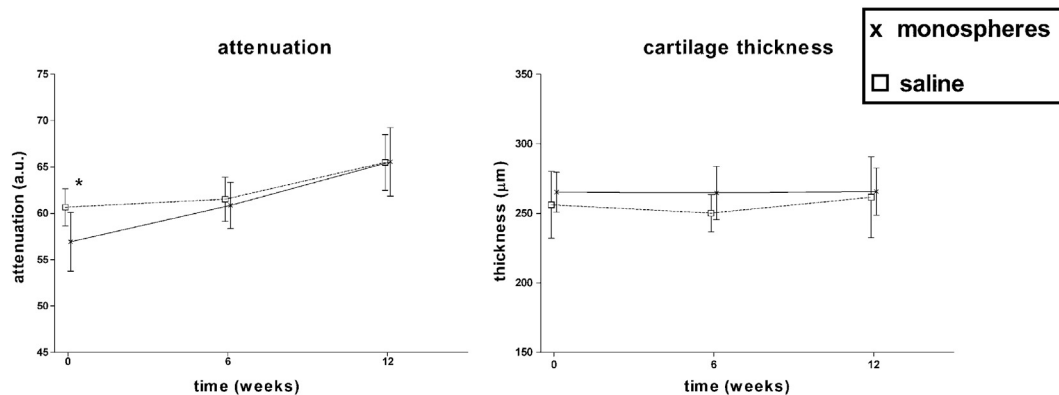


Fig. 6. Attenuation (in arbitrary units) and cartilage thickness (in μ m) of the patellar cartilage measured over time with the use of *in vivo* longitudinal μ CT arthrographies (5 μ m and 30 groups combined; n = 7 in total). No significant changes occurred during the course of 12 weeks after intra-articular injection of unloaded microspheres when compared to both baseline measurement and control knees (saline injected). * $p < 0.05$.

cartilage [55]. Neither compared to baseline nor to the contralateral control knees (saline), changes in patellar cartilage quality or quantity occurred over the full course of the experiment ($t = 6$ and 12 weeks).

3.5.2. EPIC scanning

Analysis of the rat tibial cartilage (Fig. 7-A with representative images shown in Fig. 7-B), both medial and lateral, showed that no differences were observed between the saline and monospheres injected knees with respect to either cartilage thickness or quality (sGAG content). Moreover, no surface irregularities due to possible indentation of the monospheres were seen in any of the samples. Data of EPIC scans made after unilateral osteoarthritis induction performed in a previous study by our group [55] are shown as well for comparison, showing changes in attenuation and cartilage thickness that are specifically found in rat knees affected by osteoarthritis.

3.5.3. Histology cartilage

Histology confirmed the findings of both the *in vivo* and EPIC scans. No differences in safranin O staining were found between monospheres injected rat knees (5 and 30 μm) and their controls. Also, morphologically the cartilage appeared healthy in all groups.

In Fig. 7-C, representative histological images of saline and monospheres injected knees are shown, for comparison also a diseased knee (OA) is shown with clear signs of GAG leakage and loss of cartilage thickness.

3.5.4. Histology surrounding tissue

As stated earlier, 5 μm monospheres can be taken up by synovial macrophages while 30 μm monospheres would not be phagocytized [56,57] and are therefore more likely to stay within the synovial fluid. This is indeed what was seen macroscopically after opening of injected knee joints; 5 μm monospheres were taken up already 24 h after injection while 30 μm monospheres could still be identified in the synovial fluid 4 weeks post-injection. Based on these observations, we decided to more extensively investigate the macrophage infiltration of knees injected with 5 μm monospheres at several time points. The infrapatellar folds containing the synovial membrane were harvested at several time points. Immunohistochemistry on the excised tissues surrounding the knee joint indeed showed positive CD68 staining 24 h and 4 days after intra-articular injection of the 5 μm monospheres, indicating macrophage infiltration (Fig. 7-D). More detailed analysis of the image with the highest amount of macrophages (day 4), showed that some macrophages had indeed phagocytosed monospheres.

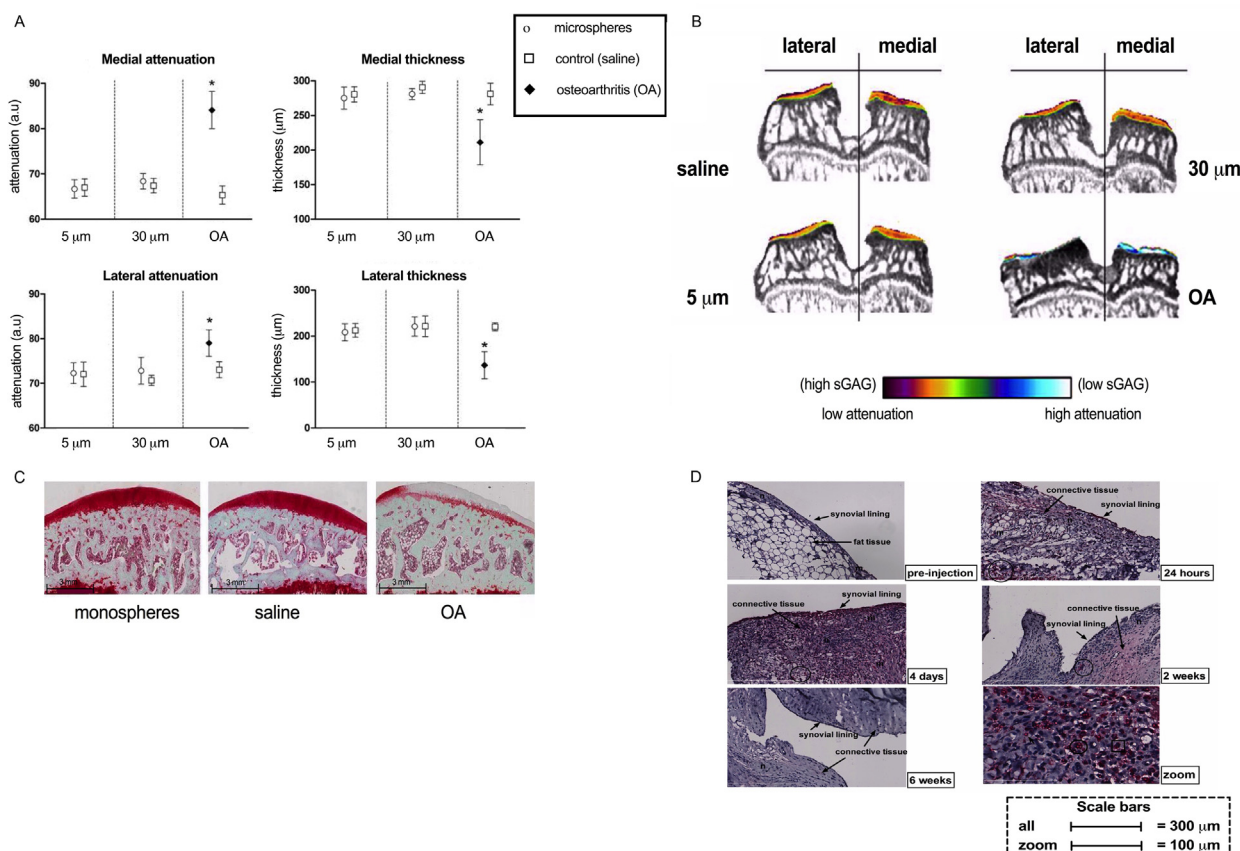


Fig. 7. A) Graphs representing cartilage quantity (thickness) and quality (attenuation) of monospheres injected knees vs. control knees (saline injected) measured with EPIC scanning. As a comparison, values of OA knees are also presented. No significant differences were found between monospheres- and saline injected knees. *: All measurements of OA knees were significantly different from both saline- and monospheres injected knees. B) Representative EPIC images of the medial and lateral tibial plateau of monospheres (5 and 30 μm) and saline injected knees 12 weeks post-injection as well as a knee with induced OA. No changes in cartilage thickness and attenuation occurred (see color scheme) in monospheres injected knees C) representative histological images of knees injected with either monospheres or saline, stained with Saf-O (cartilage in red); on the right an OA specimen. D) Histology of macrophage-staining performed on synovial tissue retrieved at different time points related to intra-articular 5 μm monospheres injection (before, after 24 h, 4 days, 2 weeks and 6 weeks). Macrophages are stained red. These images show that the presence of monospheres (which also seem to take up some of the staining) in the knee joint triggered an inflammatory macrophage reaction, which had returned to baseline at the 2 weeks time point. At all time points following the injection, neutrophils are present. Furthermore, these images show that some of the monospheres are taken up by the cells (likely macrophages) within the synovial tissue. This phenomenon did not occur yet at the 24 h time point, but was prevalent 4 days after injection (see 6x zoomed image). (For interpretation of the references to color in this figure legend, the reader is referred to the web version of this article.)

Two weeks after injection, macrophage infiltration had decreased significantly and 6 weeks after injection hardly any macrophages could be observed. At all time points after injection, some neutrophils were accumulated in the connective tissue, being most prevalent at $t = 4$ and $t = 2$ weeks.

4. Discussion

The aim of this study was to investigate the suitability of different biodegradable multi-block copolymers for the development of injectable monospheres for local intra-articular drug delivery. First of all, we tested *in vitro* which copolymer would be most suitable for this application. Different xx [PDLLA-PEG₁₀₀₀-PDLLA]- yy [PLLA] multi-block co-polymers of different composition were characterized on their composition, molecular weights and thermal properties (glass transition temperature and melting temperature/enthalpy) as well as for their *in vitro* degradation characteristics. ¹H NMR analysis confirmed that the LA/PEG molar ratios of the xx [PDLLA-PEG₁₀₀₀-PDLLA]- yy [PLLA] multi-block copolymers were in line with their feed compositions. DSC confirmed the phase-separated nature of the xx [PDLLA-PEG₁₀₀₀-PDLLA]- yy [PLLA] multi-block copolymers, showing a distinct glass transition temperature (T_g) for the PDLLA-PEG₁₀₀₀-PDLLA based amorphous domains, along with a clear melting peak for the PLLA-based crystalline domains. These crystalline domains act as physical crosslinks and control the swelling of the amorphous PEG/PDLLA phase in the polymeric material under physiological conditions. The significant decrease in T_g observed upon increasing the PDLLA-PEG₁₀₀₀-PDLLA/PLLA block ratio from 10/90 to 50/50, is caused by PEG which acts as plasticizer and reduces the T_g of the amorphous block due to its complete miscibility with amorphous PDLLA [58,59]. Although the changes in T_m were not as noticeable as in the case of T_g , the decrease in the melting enthalpy (ΔH) showed that the crystallinity of the multi-block copolymers decreased with increases of overall PEG-content in the polymer matrix (ΔH decreased from 59.8 J/g for 5 wt.% PEG-containing polymer to 16.1 J/g when 25 wt.% PEG was present). Increasing the PEG content in the polymer composition also had an impact on the swelling of the matrix (Table 2) due to the hydrophilic behavior of this polymer [60]. This could be relevant for future evaluation of drugs encapsulated within these matrices because the release of encapsulated compounds usually occurs via diffusion through the swollen polymer matrix. Furthermore, an accelerated mass loss during the initial phase of *in vitro* degradation was observed for the polymers with a higher content of the amorphous block, most probably caused by PEG loss. This is in line with our ¹H NMR measurements and with other published studies on PEG-containing block co-polymers, where PEG preferentially leaves the material during early stages of degradation due to preferential cleavage of the ester bonds that connects PEG and the amorphous polyester block [61–64]. Although a residual amount of tin octanoate was still present in the multiblock co-polymers, it was not expected to have a detrimental effect during *in vivo* studies since it is below the maximum parenteral exposure established by the ICH guidelines (640 µg/day) [65].

For *in vivo* evaluation of differently sized monospheres, the 20 [PDLLA-PEG₁₀₀₀-PDLLA]-80[PLLA] multi-block co-polymer was chosen because it presented little degradation during the first weeks, allowing release of potentially encapsulated drugs, and a second phase of accelerated degradation, which would facilitate the elimination of the monospheres from the treated joint. Besides, this polymer contains 10% PEG, making it soft enough for intra-articular use and a potential carrier for the sustained release of hydrophobic small drug molecules (MW 350–1000 g/mole) that are typically used for OA treatment such as steroid

and non-steroid anti-inflammatory drugs [10,54,66]. We previously tested the mechanical compatibility of these monospheres with the cartilage. In short, the average Young's moduli of the materials in the swollen state are within the same range as the mechanical properties of healthy bovine cartilage and human osteoarthritic cartilage [31,67]. This indicates that the presence of this type of monospheres within the joint would not be likely to cause cartilage damage due to surface indentation or grinding. Furthermore, the total water uptake and thus mechanical properties can be customized depending on the needs of any target tissue by simply changing the PEG content of the monospheres. The selected 20[PDLLA-PEG₁₀₀₀-PDLLA]-80[PLLA] multi-block copolymer was used to make microspheres of 3 different sizes with the use of the microsieve membrane emulsification process. Size uniformity was reached for all batches (target particle size of 5, 15 and 30 µm), as shown in Fig. 2-A and B. These results confirm the suitability of this process to prepare monospheres with well-defined size and with a narrow particle size distribution. As stated before, narrow particle size distribution allows the use of smaller needles and consequently less painful injections. Indeed, monosphere suspensions were well injectable through a 27G needle at concentrations up to 25% wt. (data not shown). Furthermore, the absence of very small microspheres could avoid particle-induced immunoactivation [18] and size uniformity allows more reproducible and predictable *in vivo* release kinetics [30,31].

It is very important for a drug delivery system specifically designed for intra-articular use to be able to stay within the injected joint long enough to fully release the loaded drug locally, and in a timescale where it could potentially be effective for joint repair and/or pain relief. *In vitro* evaluation of the monospheres under the above described accelerated conditions retained the dye up to 10 days, which could be translated to approximately 80 days under physiological conditions. In short, an experiment was performed to determine whether the dye is retained in the monospheres during degradation.

Real time (37 °C, pH7.4) degradation testing shows the presence of microspheres after 80 days [68,69]. This was confirmed by the *in vivo* experiments on tissue surrounding the equine middle carpal joint. We also showed the potential of 5, 15 and 30 µm monospheres to remain intra-articular for at least 3 months, allowing the monospheres to act as a sustained local drug delivery system. After showing that the monospheres remained in the injected joints for a period long enough to release any encapsulated drug, we extensively tested the intra-articular biocompatibility of the monospheres. This is a very important part in the fabrication of any intra-articular drug delivery system, since the drug carrier intended to treat joint diseases like osteoarthritis should clearly not lead to negative effects in the joint upon intra-articular application. In horses, the intra-articular injection of unloaded monospheres gave rise to a mild transient inflammatory response, shown by a significant increase of WBC and total protein content in the synovial fluid (Fig. 5-A) of 72 h and thereafter returned to baseline level quickly. A similar transient inflammatory reaction has been shown previously after intra-articular injection of hyaluronic acid (HA), a regulatory approved and widely used clinical treatment option in equine and human OA [70–72]. In fact, intra-articular injection of HA lead to an inflammatory response that is severe enough to cause transient lameness in horses, a reaction that is clinically known as a “flare” [73], a phenomenon that was clearly not present after injection of 30 µm [20PDLLA-PEG1000-PDLLA]-80[PLLA] monospheres. This comparison therefore shows that the use of monospheres compares favorably with current clinical practice and can be considered safe for intra-articular use. It has been suggested that chronic inflammation plays an important

role in the development of structural changes seen in osteoarthritis, since activated macrophages produce enzymes, growth factors and cytokines that will negatively affect joint structures like synovium, bone and cartilage [74]. Therefore, it was important to determine whether the inflammatory reaction followed by the intra-articular injection of monospheres had any deleterious effect on the joints. In order to do so, we first measured GAG content and C2C epitope (a neoepitope present on collagenase-cleavage fragments of type II collagen, hence a catabolic marker [75]) in the synovial fluid samples (Fig. 5-C). An increase of these markers in the synovial fluid would indicate cartilage breakdown. The significant differences observed at baseline are most likely due to (small) differences in status of the joints due to the age and amount of exercise of the horses in the past, although the horses were all declared healthy based on X-ray before starting the experiments. GAG release into the SF remained at or below baseline values during the whole experiment, indicating that no loss of GAGs (an early sign of cartilage damage and OA) occurred due to the presence of intra-articular monospheres. Moreover, our values were approximately 10-fold lower compared to inflamed horse joints after LPS injection of around 300 µg/ml [46], all of our values remained in the range of values found for healthy joints. The C2C content has shown to be elevated in rheumatoid arthritis and OA when there is damage to the cartilage [76], more specifically it indicates an inflammation-induced enhancement of collagen II cleavage [77]. In our study this was clearly not the case, as there was no increase in C2C content at any time point (Fig. 5-D).

In theory, both 5 and 30 µm monospheres could have negative effects on cartilage, however via different mechanisms. Five µm monospheres can be taken up by synovial macrophages [13,56,57] which could potentially give rise to an inflammatory reaction, while 30 µm monospheres would not be phagocytized and therefore be more likely to stay within the synovial fluid, but with the potential risk of friction or indentation of the cartilage surface. Based on the equine SF analysis (Section 3.2), we had strong indications to believe that the presence of monospheres within a joint does not harm the cartilage. To verify this assumption, 12 healthy rats were used to more accurately test the intra-articular biocompatibility of the unloaded 5 and 30 µm 20[PDLLA-PEG₁₀₀₀-PDLLA]-80[PLLA] monospheres compared to contra-lateral saline injections. Using *in vivo* µCT scanning (Fig. 6), followed by EPIC scans to even more accurately quantify cartilage thickness and quality (Fig. 7-A,B) and histology (Fig. 7-C), we indeed showed that no changes on cartilage thickness or cartilage quality (attenuation) occurred. The macrophage infiltration seen in the tissue surrounding the knees injected with monospheres (Fig. 7-D) correlates very well with the mild transient reaction in the first 2 weeks seen in the equine synovial fluid samples. The recruitment of macrophages and neutrophils following the intra-articular injection of a foreign material is considered physiological. Moreover, in the case of our monospheres it did not lead to any negative effects (as indicated by both µCT-scanning and histology of the injected joints). These findings show that monospheres composed of [PDLLA-PEG₁₀₀₀-PDLLA]-[PLLA] multi-block copolymers are safe for intra-articular use. Recruitment of macrophages is one of the 5 phases of a foreign body response. These phases are: protein absorption, acute and chronic inflammation, foreign body giant cell formation and fibrosis [78]. The formation of fibrosis is an undesirable feature, since this would prevent drug release from the monospheres. More importantly, fibrosis within a joint lead to pain and loss of function. Joint capsules consist of a dense fibrous connective tissue, lined with synovium, surrounding the joint. Therefore, it would be difficult to quantify fibrosis due to a foreign body reaction. The second phase of the foreign body reaction -acute

inflammation- was seen in our horse study (significant increase of WBC and total protein count), as well as our rat study (presence of macrophages and neutrophils). Chronic inflammation was not the case for either of the animal models and the inflammatory response had returned to baseline 2 weeks post-injection. Additionally, no foreign body giant cell formation was observed at any time point. Therefore, the formation of a fibrous capsule is not very likely since this would follow chronic inflammation. Also, based on literature we know that adding PLLA to PEG largely reduced (90% reduction) capsule formation [79]. Another study, in which 5, 15 and 30 µm monospheres were injected subcutaneously, no capsule formation was observed up until the end-point at 28 days post-injection [80].

Very interestingly, we see a portion of our monospheres being taken up by macrophages in the synovium (Fig. 7-D). In this current study, we only investigated the synovium of joint injected with 5 µm monospheres. From literature, we know that 5–10 µm is optimal for macrophage phagocytosis [66], because phagocytosis is ensured and therefore a prolonged retention in the joint is achieved. It has been suggested that phagocytosis ensures lower drug-exposure to the cartilage and hence less change of negative side-effect [81]; however, this assumption is not proven in this cited study nor has it, to our knowledge, been proven by other authors. It is also debatable, whether or not direct exposure of cartilage to a drug would necessarily have a negative outcome. Depending on the application and the type of drug encapsulated, one might opt for a different size of monospheres. For instance, when directly acting on inflammatory reactions, 5 µm monospheres might be preferable due to phagocytosis. It has been suggested that macrophages play an important role in the development of OA [82]. When macrophages become activated, they are able to produce a variety of enzymes [83], growth factors [84], and pro-inflammatory cytokines such as TNFα and interleukins [85,86]. These, and other macrophage products play a major role in the OA development and may maintain the vicious circle by acting on the formation of synovial fibrosis and further induce the inflammatory state of the affected joint that leads to cartilage destruction [83,87]. Injection of 5 µm monospheres containing an anti-inflammatory drug would therefore not only lead to a sustained local release of the drug, but might even lead to a more targeted effect on the local macrophages, thereby breaking the vicious circle of OA [13]. In contrast, when a drug that specifically acts on chondrocytes is injected, it would be reasonable to choose for larger monospheres (15 or 30 µm). From our current study, it can be concluded that the different sizes evaluated (5, 15, 30 µm) present equal levels of joint retention and biocompatibility. Therefore, the selection of the optimal size for intra-articular use should be based on the cells to be targeted.

5. Conclusion

Monospheres of different sizes (5, 15 and 30 µm) composed of biodegradable [PDLLA-PEG₁₀₀₀-PDLLA]-*b*-[PLLA] multi-block copolymers were successfully obtained using a membrane emulsification process. Following intra-articular injection, both small (5 µm) and larger (30 µm) monospheres remained present in the joints of both small (mice and rats) and large animals (horses) for up to 3 months, which is likely long enough to release an incorporated drug. The monospheres elicited a mild transient inflammatory reaction similar to clinically used injectables, and did not harm the cartilage in any way in either of these animals. The excellent biocompatibility combined with the desirable intra-articular retention show that [PDLLA-PEG₁₀₀₀-PDLLA]-*b*-[PLLA] monospheres have great potential as intra-articular drug delivery system for the treatment of arthritic diseases.

Acknowledgment

This research forms part of the Project P2.02 OAcontrol of the research program of the BioMedical Materials institute, co-funded by the Dutch Ministry of Economic Affairs, Agriculture and Innovation.

This work was supported by the Dutch Arthritis Foundation (LLP-22).

Nanomi B.V. is acknowledged for providing the Microsieve Emulsification Technology.

Appendix A. Supplementary data

Supplementary data associated with this article can be found, in the online version, at <http://dx.doi.org/10.1016/j.actbio.2016.11.003>.

References

- [1] E. Odding, H.A. Valkenburg, H.J. Stam, A. Hofman, Determinants of locomotor disability in people aged 55 years and over: the Rotterdam Study, *Eur. J. Epidemiol.* 17 (2001) 1033–1041.
- [2] Recommendations for the medical management of osteoarthritis of the hip and knee: 2000 update. American College of Rheumatology Subcommittee on Osteoarthritis Guidelines. *Arthritis and Rheumatism* 2000;43:1905–15.
- [3] Z. Zhang, X. Bi, H. Li, G. Huang, Enhanced targeting efficiency of PLGA microspheres loaded with Lornoxicam for intra-articular administration, *Drug Delivery* 18 (2011) 536–544.
- [4] R.O. Day, A.J. McLachlan, G.G. Graham, K.M. Williams, Pharmacokinetics of nonsteroidal anti-inflammatory drugs in synovial fluid, *Clin. Pharmacokinet.* 36 (1999) 191–210.
- [5] W.J. Wallis, P.A. Simkin, Antirheumatic drug concentrations in human synovial fluid and synovial tissue. Observations on extravascular pharmacokinetics, *Clin. Pharmacokinet.* 8 (1983) 496–522.
- [6] S.H. Roth, S. Anderson, The NSAID dilemma: managing osteoarthritis in high-risk patients, *Phys. Sportsmed.* 39 (2011) 62–74.
- [7] N. Bellamy, J. Campbell, V. Robinson, T. Gee, R. Bourne, G. Wells, Intraarticular corticosteroid for treatment of osteoarthritis of the knee, *Cochrane Database Syst. Rev.* (2006). CD005328.
- [8] D.J. Hunter, In the clinic. Osteoarthritis, *Ann. Intern. Med.* 147 (2007). ITC8-1–ITC8-16.
- [9] C. Bahadir, B. Onal, V.Y. Dayan, N. Gurer, Comparison of therapeutic effects of sodium hyaluronate and corticosteroid injections on trapeziometacarpal joint osteoarthritis, *Clin. Rheumatol.* 28 (2009) 529–533.
- [10] M.L. Kang, G.I. Im, Drug delivery systems for intra-articular treatment of osteoarthritis, *Expert Opin. Drug Del.* 11 (2014) 269–282.
- [11] M. Fazil, A. Ali, S. Baboota, J.K. Sahni, J. Ali, Exploring drug delivery systems for treating osteoporosis, *Expert Opin. Drug Del.* 10 (2013) 1123–1136.
- [12] C. Larsen, J. Ostergaard, S.W. Larsen, H. Jensen, S. Jacobsen, C. Lindegaard, P.H. Andersen, Intra-articular depot formulation principles: role in the management of postoperative pain and arthritic disorders, *J. Pharm. Sci. U.S.* 97 (2008) 4622–4654.
- [13] S.H.R. Edwards, Intra-articular drug delivery: the challenge to extend drug residence time within the joint, *Vet. J.* 190 (2011) 15–21.
- [14] N. Gerwin, C. Hops, A. Lucke, Intraarticular drug delivery in osteoarthritis, *Adv. Drug Deliv. Rev.* 58 (2006) 226–242.
- [15] M.J. Sandker, A. Petit, E.M. Redout, M. Siebelt, B. Muller, P. Bruin, R. Meyboom, T. Vermonden, W.E. Hennink, H. Weinans, In situ forming acyl-capped PCLA-PEG-PCL triblock copolymer based hydrogels, *Biomaterials* 34 (2013) 8002–8011.
- [16] K. Fu, D.W. Pack, A.M. Klibanov, R. Langer, Visual evidence of acidic environment within degrading poly(lactic-co-glycolic acid) (PLGA) microspheres, *Pharm. Res.* 17 (2000) 100–106.
- [17] A. Shenderova, T.G. Burke, S.P. Schwendeman, The acidic microclimate in poly(lactide-co-glycolide) microspheres stabilizes camptothecins, *Pharm. Res.* 16 (1999) 241–248.
- [18] A. Giteau, M.C. Venier-Julienne, S. Marchal, J.L. Courthaudon, M. Sergeant, C. Montero-Menei, J.M. Verdier, J.P. Benoit, Reversible protein precipitation to ensure stability during encapsulation within PLGA microspheres, *Eur. J. Pharm. Biopharm.* 70 (2008) 127–136.
- [19] B.S. Zolnik, D.J. Burgess, Effect of acidic pH on PLGA microsphere degradation and release, *J. Control Release* 122 (2007) 338–344.
- [20] M.S. Shive, J.M. Anderson, Biodegradation and biocompatibility of PLA and PLGA microspheres, *Adv. Drug Deliv. Rev.* 28 (1997) 5–24.
- [21] H. Thakkar, R.K. Sharma, A.K. Mishra, K. Chuttani, R.S.R. Murthy, Celecoxib incorporated chitosan microspheres: in vitro and in vivo evaluation, *J. Drug Target* 12 (2004) 549–557.
- [22] S.R. Mao, C.Q. Guo, Y. Shi, L.C. Li, Recent advances in polymeric microspheres for parenteral drug delivery-part 2, *Expert Opin. Drug Del.* 9 (2012) 1209–1223.
- [23] S.R. Mao, C.Q. Guo, Y. Shi, L.C. Li, Recent advances in polymeric microspheres for parenteral drug delivery – part 1, *Expert Opin. Drug Del.* 9 (2012) 1161–1176.
- [24] Y.Y. Yang, H.H. Chia, T.S. Chung, Effect of preparation temperature on the characteristics and release profiles of PLGA microspheres containing protein fabricated by double-emulsion solvent extraction/evaporation method, *J. Control Release* 69 (2000) 81–96.
- [25] V.T. Tran, J.P. Benoit, M.C. Venier-Julienne, Why and how to prepare biodegradable, monodispersed, polymeric microparticles in the field of pharmacy?, *Int. J. Pharm.* 407 (2011) 1–11.
- [26] F. Ito, H. Fujimori, H. Honnami, H. Kawakami, K. Kanamura, K. Makino, Study of types and mixture ratio of organic solvent used to dissolve polymers for preparation of drug-containing PLGA microspheres, *Eur. Polym. J.* 45 (2009) 658–667.
- [27] T.S.M. Nakashima, M. Kukizaki, Membrane emulsification by microporous glass, *Key Eng. Mater.* 513 (1991) 61–62.
- [28] T. Nakashima, M. Shimizu, M. Kukizaki, Particle control of emulsion by membrane emulsification and its applications, *Adv. Drug Deliv. Rev.* 45 (2000) 47–56.
- [29] W. Rungseewijitprapa, R. Bodmeier, Injectability of biodegradable in situ forming microparticle systems (ISM), *Eur. J. Pharm. Sci.* 36 (2009) 524–531.
- [30] J.C. De La Vega, P. Elischer, T. Schneider, U.O. Hafeli, Uniform polymer microspheres: monodispersity criteria, methods of formation and applications, *Nanomedicine (Lond)* 8 (2013) 265–285.
- [31] J. Siepmann, N. Faisant, J. Akiki, J. Richard, J.P. Benoit, Effect of the size of biodegradable microparticles on drug release: experiment and theory, *J. Control Release* 96 (2004) 123–134.
- [32] J.F.Q. Wu, Y. Xia, G. Ma, Uniform-sized particles in biomedical field prepared by membrane emulsification technique, *Chem. Eng. Sci.* 125 (2015) 85–97.
- [33] F. Kazazi-Hyseni, M. Landin, A. Lathuile, G.J. Veldhuis, S. Rahimian, W.E. Hennink, R.J. Kok, C.F. van Nostrum, Computer modeling assisted design of monodisperse PLGA microspheres with controlled porosity affords zero order release of an encapsulated macromolecule for 3 months, *Pharm. Res.* 31 (2014) 2844–2856.
- [34] F. Ramazani, C. Hiemstra, R. Steendam, F. Kazazi-Hyseni, C.F. Van Nostrum, G. Storm, F. Kiessling, T. Lammers, W.E. Hennink, R.J. Kok, Sunitinib microspheres based on [PDLLA-PEG-PDLLA]-b-PLLA multi-block copolymers for ocular drug delivery, *Eur. J. Pharm. Biopharm.* 95 (2015) 368–377.
- [35] Hissink CE. In: patent P, editor. 2004.
- [36] L. Li, S.P. Schwendeman, Mapping neutral microclimate pH in PLGA microspheres, *J. Control Release* 101 (2005) 163–173.
- [37] Y.J. Liu, S.P. Schwendeman, Mapping microclimate pH distribution inside protein-encapsulated PLGA microspheres using confocal laser scanning microscopy, *Mol. Pharmaceut.* 9 (2012) 1342–1350.
- [38] J.P. Caron, R.L. Genovese, Principles and practices of joint disease treatment, in: M.W.D.S. Ross (Ed.), *Diagnosis and Management of Lameness in the Horse*, Elsevier, Philadelphia, 2003, pp. 746–764.
- [39] J.P., Caron, R.L., Genovese, 2000, United States Department of Agriculture. Lameness and laminitis in U.S. Horses. National Animal Health Monitoring System.
- [40] G. Nilsson, S.E. Olsson, Radiologic and patho-anatomic changes in the distal joints and the phalanges of the standardbred horse, *Acta Vet Scand Suppl.* 44 (1973) 1–57.
- [41] C.W. McIlwraith, D.D. Frisbie, C.E. Kawcak, The horse as a model of naturally occurring osteoarthritis, *Bone Joint Res.* 1 (2012) 297–309.
- [42] M.H. Gregory, N. Capito, K. Kuroki, A.M. Stoker, J.L. Cook, S.L. Sherman, A review of translational animal models for knee osteoarthritis, *Arthritis* 2012 (2012) 764621.
- [43] M. Stankovic, H. de Waard, R. Steendam, C. Hiemstra, J. Zuidema, H.W. Frijlink, W.L. Hinrichs, Low temperature extruded implants based on novel hydrophilic multiblock copolymer for long-term protein delivery, *Eur. J. Pharm. Sci.* 49 (2013) 578–587.
- [44] G.K. Lindsay, P.F. Roslansky, T.J. Novitsky, Single-step, chromogenic limulus amoebocyte lysate assay for endotoxin, *J. Clin. Microbiol.* 27 (1989) 947–951.
- [45] M.W. Ross, The lameness score: quantification of lameness severity, in: S.J.D., editor, *Diagnosis and Management of Lameness in the Horse*. Philadelphia: W. B. Saunders, 2003. p. 66–7.
- [46] J.C. de Grauw, C.H. van de Lest, P.A. Brama, B.P. Rambags, P.R. van Weeren, In vivo effects of meloxicam on inflammatory mediators, MMP activity and cartilage biomarkers in equine joints with acute synovitis, *Equine Vet. J.* 41 (2009) 693–699.
- [47] M. Siebelt, J.H. Waarsing, N. Kops, T.M. Pijlsma, J.A.N. Verhaar, E.H.G. Oei, H. Weinans, Quantifying osteoarthritic cartilage changes accurately using in vivo MicroCT arthrography in three etiologically distinct rat models, *J. Orthop. Res.* 29 (2011) 1788–1794.
- [48] T.M. Pijlsma, J.H. Waarsing, N. Kops, P. Pavljasevic, J.A.N. Verhaar, G.J.V.M. van Osch, H. Weinans, In vivo imaging of cartilage degeneration using mu CT-arthrography, *Osteoarthr. Cartilage* 16 (2008) 1011–1017.
- [49] T.S. Silvest, J.S. Jurvelin, A.S. Aula, M.J. Lammi, J. Toyras, Contrast agent-enhanced computed tomography of articular cartilage: association with tissue composition and properties, *Acta Radiol.* 50 (2009) 78–85.
- [50] T.S. Silvest, J.S. Jurvelin, M.J. Lammi, J. Toyras, PQCT study on diffusion and equilibrium distribution of iodinated anionic contrast agent in human articular cartilage—associations to matrix composition and integrity, *Osteoarthritis Cartilage* 17 (2009) 26–32.

- [51] A.W. Palmer, R.E. Guldberg, M.E. Levenston, Analysis of cartilage matrix fixed charge density and three-dimensional morphology via contrast-enhanced microcomputed tomography, *Proc. Natl. Acad. Sci. U. S. A.* 103 (2006) 19255–19260.
- [52] J.H. Waarsing, J.S. Day, H. Weinans, An improved segmentation method for in vivo μ CT Imaging, *J. Bone Miner. Res.* 19 (2004) 1640–1650.
- [53] R. Kumar, M.J. Palmieri, Points to consider when establishing drug product specifications for parenteral microspheres, *Aaps J.* 12 (2010) 27–32.
- [54] A. Petit, E.M. Redout, C.H. van de Lest, J.C. de Grauw, B. Muller, R. Meyboom, P. van Midwoud, T. Vermonden, W.E. Hennink, P.R. van Weeren, Sustained intra-articular release of celecoxib from in situ forming gels made of acetyl-capped PCL-PEG-PCL triblock copolymers in horses, *Biomaterials* 53 (2015) 426–436.
- [55] M. Siebelt, H.C. Groen, S.J. Koelewijn, E. de Blois, M. Sandker, J.H. Waarsing, C. Müller, G.J. van Osch, M. de Jong, H. Weinans, Increased physical activity severely induces osteoarthritic changes in knee joints with papain induced sulphate-glycosaminoglycan depleted cartilage, *Arthritis Res. Ther.* 16 (2014) R32.
- [56] R.L. Illgen, T.M. Forsythe, J.W. Pike, M.P. Laurent, C.R. Blanchard, Highly crosslinked vs conventional polyethylene particles – an in vitro comparison of biologic activities, *J. Arthroplasty* 23 (2008) 721–731.
- [57] T.R. Green, J. Fisher, M. Stone, B.M. Wroblewski, E. Ingham, Polyethylene particles of a 'critical size' are necessary for the induction of cytokines by macrophages in vitro, *Biomaterials* 19 (1998) 2297–2302.
- [58] C.G. Mothe, A.D. Azevedo, W.S. Drummond, S.H. Wang, Thermal properties of amphiphilic biodegradable triblock copolymer of L, L-lactide and ethylene glycol, *J. Therm. Anal. Calorim.* 101 (2010) 229–233.
- [59] S.Y. Lee, I.J. Chin, J.S. Jung, Crystallization behavior of poly(L-lactide)-poly(ethylene glycol) multiblock copolymers, *Eur. Polym. J.* 35 (1999) 2147–2153.
- [60] J.E. Kim, S.R. Kim, S.H. Lee, C.H. Lee, D.D. Kim, The effect of pore formers on the controlled release of cefadroxil from a polyurethane matrix, *Int. J. Pharm.* 201 (2000) 29–36.
- [61] A. Petit, B. Muller, R. Meijboom, P. Bruin, F. van de Manakker, M. Versluis-Helder, L.G.J. de Leede, A. Doornbos, M. Landin, W.E. Hennink, T. Vermonden, Effect of Polymer Composition on Rheological and Degradation Properties of Temperature-Responsive Gelling Systems Composed of Acyl-Capped PCL-PEG-PCL, *Biomacromolecules* 14 (2013) 3172–3182.
- [62] M.G. Carstens, C.F. van Nostrum, R. Verrijck, L.G.J. De Leede, D.J.A. Crommelin, W.E. Hennink, A mechanistic study on the chemical and enzymatic degradation of PEG-Oligo(ϵ -caprolactone) micelles, *J. Pharm. Sci.-Us* 97 (2008) 506–518.
- [63] M.H. Huang, S.M. Li, D.W. Huttmacher, J.T. Schantz, C.A. Vacanti, C. Braud, M. Vert, Degradation and cell culture studies on block copolymers prepared by ring opening polymerization of ϵ -caprolactone in the presence of poly(ethylene glycol), *J. Biomed. Mater. Res. A* 69A (2004) 417–427.
- [64] M.L. Zweers, G.H. Engbers, D.W. Grijpma, J. Feijen, In vitro degradation of nanoparticles prepared from polymers based on DL-lactide, glycolide and poly(ethylene oxide), *J. Control Release* 100 (2004) 347–356.
- [65] ICH. ICH guidelines. http://www.ich.org/fileadmin/Public_Web_Site/ICH_Products/Guidelines/Quality/Q3D/Q3D_Step_4.pdf 2014.
- [66] N. Butoescu, O. Jordan, E. Doelker, Intra-articular drug delivery systems for the treatment of rheumatic diseases: a review of the factors influencing their performance, *Eur. J. Pharm. Biopharm.* 73 (2009) 205–218.
- [67] P.R. Moshtagh, J. Rauker, M.J. Sandker, M.R. Zuiddam, F.W.A. Dirne, E. Klijnstra, L. Duque, R. Steendam, H. Weinans, A.A. Zadpoor, Nanomechanical properties of multi-block copolymer microspheres for drug delivery applications, *J. Mech. Behav. Biomed.* 34 (2014) 313–319.
- [68] K. Makino, M. Arakawa, T. Kondo, Preparation and in vitro degradation properties of polylactide microcapsules, *Chem. Pharm. Bull. (Tokyo)* 33 (1985) 1195–1201.
- [69] S.S. D'Souza, J.A. Faraj, P.P. DeLuca, 2005, A model-dependent approach to correlate accelerated with real-time release from biodegradable microspheres, *Aaps Pharmscitec.*, 6.
- [70] D.W. Jackson, T.M. Simon, Intra-articular distribution and residence time of Hyal A and B: a study in the goat knee, *Osteoarthritis Cartilage* 14 (2006) 1248–1257.
- [71] M. Adams, Viscosupplementation as an alternative to conventional treatment for the management of osteoarthritis of the knee, *Jcr-J. Clin. Rheumatol.* 5 (1999) S18–S23.
- [72] A. Lussier, A.A. Cividino, C.A. McFarlane, W.P. Olszynski, W.J. Potashner, R. DeMedicis, Viscosupplementation with hyal for the treatment of osteoarthritis: findings from clinical practice in Canada, *J. Rheumatol.* 23 (1996) 1579–1585.
- [73] L.A. Fortier, 2005, Systemic therapies for joint disease in horses, *The Veterinary clinics of North America Equine practice*, 21, 547–57, v. .
- [74] J.P. Pelletier, J. Martel-Pelletier, S.B. Abramson, Osteoarthritis, an inflammatory disease – potential implication for the selection of new therapeutic targets, *Arthritis Rheum.* 44 (2001) 1237–1247.
- [75] T. Kojima, F. Mwale, T. Yasuda, C. Girard, A.R. Poole, S. Laverty, Early degradation of type IX and type II collagen with the onset of experimental inflammatory arthritis, *Arthritis Rheum.* 44 (2001) 120–127.
- [76] K.A. Elsaid, C.O. Chichester, Review: collagen markers in early arthritic diseases, *Clin. Chim. Acta* 365 (2006) 68–77.
- [77] A. Fraser, U. Fearon, R.C. Billingham, M. Ionescu, R. Reece, T. Barwick, P. Emery, A.R. Poole, D.J. Veale, Turnover of type II collagen and aggrecan in cartilage matrix at the onset of inflammatory arthritis in humans – relationship to mediators of systemic and local inflammation, *Arthritis Rheum.* 48 (2003) 3085–3095.
- [78] R. Klopfeisch, Macrophage reaction against biomaterials in the mouse model – Phenotypes, functions and markers, *Acta Biomater.* (2016).
- [79] T. Ehashi, S. Kakinoki, T. Yamaoka, Water absorbing and quick degradable PLLA/PEG multiblock copolymers reduce the encapsulation and inflammatory cytokine production, *J. Artif. Organs* 17 (2014) 321–328.
- [80] J. Zandstra, C. Hiemstra, A.H. Petersen, J. Zuidema, M.M. van Beuge, S. Rodriguez, A.A. Lathuile, G.J. Veldhuis, R. Steendam, R.A. Bank, E.R. Popa, Microsphere size influences the foreign body reaction, *Eur. Cell Mater.* 28 (2014) 335–347.
- [81] J.H. Ratcliffe, I.M. Hunneyball, C.G. Wilson, A. Smith, S.S. Davis, Albumin microspheres for intra-articular drug delivery: investigation of their retention in normal and arthritic knee joints of rabbits, *J. Pharm. Pharmacol.* 39 (1987) 290–295.
- [82] J. Bondeson, A.B. Blom, S. Wainwright, C. Hughes, B. Caterson, W.B. van den Berg, The role of synovial macrophages and macrophage-produced mediators in driving inflammatory and destructive responses in osteoarthritis, *Arthritis Rheum.* 62 (2010) 647–657.
- [83] A.B. Blom, P.L. Lent, S. Libregts, A.E. Holthuysen, P.M. van der Kraan, N. van Rooijen, W.B. van den Berg, Crucial role of macrophages in matrix metalloproteinase-mediated cartilage destruction during experimental osteoarthritis – involvement of matrix metalloproteinase 3, *Arthritis Rheum.* 56 (2007) 147–157.
- [84] E.N.B. Davidson, E.L. Vitters, F.M. Mooren, N. Oliver, W.B. van den Berg, P.M. van der Kraan, Connective tissue growth factor/CCN2 overexpression in mouse synovial lining results in transient fibrosis and cartilage damage, *Arthritis Rheum.* 54 (2006) 1653–1661.
- [85] L.I. Sakka, N.A. Johanson, C.R. Scanzello, C.D. Platoucas, Interleukin-12 is expressed by infiltrating macrophages and synovial lining cells in rheumatoid arthritis and osteoarthritis, *Cell Immunol* 188 (1998) 105–110.
- [86] M.K. Haynes, E.L. Hume, J.B. Smith, Phenotypic characterization of inflammatory cells from osteoarthritic synovium and synovial fluids, *Clin. Immunol.* 105 (2002) 315–325.
- [87] M.B. Goldring, S.R. Goldring, Osteoarthritis, *J. Cell Physiol.* 213 (2007) 626–634.